The Plant Cell, Vol. 12, 2395–2408, December 2000, www.plantcell.org © 2000 American Society of Plant Physiologists

Cloning and Characterization of *IAR1*, a Gene Required for Auxin Conjugate Sensitivity in Arabidopsis

Jamie Lasswell,[1] Luise E. Rogg, David C. Nelson,[2] Catherine Rongey,[3] and Bonnie Bartel[4]

Department of Biochemistry and Cell Biology, Rice University, Houston, Texas 77005-1892

Most indole-3-acetic acid (IAA) in higher plants is conjugated to amino acids, sugars, or peptides, and these conjugates are implicated in regulating the concentration of the free hormone. We identified *iar1* as an Arabidopsis mutant that is resistant to the inhibitory effects of several IAA–amino acid conjugates but remains sensitive to free IAA. *iar1* partially suppresses phenotypes of a mutant that overproduces IAA, suggesting that *IAR1* participates in auxin metabolism or response. We used positional information to clone *IAR1*, which encodes a novel protein with seven predicted transmembrane domains and several His-rich regions. IAR1 has homologs in other multicellular organisms, including Drosophila, nematodes, and mammals; in addition, the mouse homolog KE4 can functionally substitute for IAR1 in vivo. IAR1 also structurally resembles and has detectable sequence similarity to a family of metal transporters. We discuss several possible roles for IAR1 in auxin homeostasis.

INTRODUCTION

Indole-3-acetic acid (IAA) is the major endogenous auxin and participates in many plant developmental processes, including cell enlargement and division, differentiation of vascular tissue, initiation of lateral roots, apical dominance, and responses to environmental stimuli such as gravity and light (reviewed by Estelle and Klee, 1994; Bennett et al., 1998). Plants contain little free IAA; most IAA is found conjugated to amino acids, peptides, sugars, or high molecular weight glycans. These conjugates have been implicated in such processes as storage, transport, and protection from oxidative degradation (reviewed in Cohen and Bandurski, 1982; Bandurski et al., 1995). Plants apparently also permanently inactivate excess IAA by conjugation (reviewed in Normanly, 1997). For example, many plants form IAA-Asp as an intermediate in IAA catabolism (Tsurumi and Wada, 1986; Monteiro et al., 1988; Tuominen et al., 1994; Östin et al., 1998).

Conjugation and hydrolysis of conjugates are probable mechanisms used to regulate the concentrations of free IAA (reviewed in Normanly and Bartel, 1999), and characterization of the genes involved in these processes is a prerequisite to understanding this regulation. Although diverse land plants conjugate IAA to glucose and other molecules (Sztein et al., 1995, 1999), the only plant gene so involved that has been identified is the maize *iaglu* gene, which encodes an enzyme esterifying IAA to glucose (Szerszen et al., 1994). Various plants hydrolyze IAA conjugates, and IAA-glucose hydrolases have been identified in maize, potato, oat, and bean (Kowalczyk and Bandurski, 1990; Jakubowska et al., 1993). IAA-Ala hydrolases have been partially purified from bean and carrot (Cohen et al., 1988; Kuleck and Cohen, 1993), and Chinese cabbage extracts contain isoenzymes that hydrolyze IAA-Ala, IAA-Asp, and IAA-Phe (Ludwig-Müller et al., 1996).

The ability of several IAA conjugates to mimic the effects of free IAA on plant growth (reviewed by Bartel, 1997) has been exploited to identify Arabidopsis mutants that respond abnormally to IAA conjugates. The *ilr1* (IAA-Leu–resistant) mutant elongates roots at concentrations of IAA-Leu that inhibit wild-type root growth. The gene defective in *ilr1* encodes an amidohydrolase with high affinity for IAA-Leu and IAA-Phe and lesser affinity for IAA-Ala, IAA-Gly, and IAA-Val (Bartel and Fink, 1995). Four *ILR1*-like genes, *ILL1*, *ILL2* (Bartel and Fink, 1995), *ILL3*, and *ILL5* (Davies et al., 1999), have been identified on the basis of their similarity to *ILR1*. A sixth member of this gene family is defective in the *iar3* (IAA-Ala–resistant) mutant and encodes an amidohydrolase specific for IAA-Ala (Davies et al., 1999). Two other mutants, *icr1* and *icr2*, are resistant to growth inhibition by IAA-Phe, IAA-Ala, and IAA-Gly (Campanella et al., 1996), but the genes defective in these mutants remain unidentified.

We have been identifying and characterizing Arabidopsis mutants with altered responses to IAA–amino acid conjugates to elucidate the role of conjugate metabolism in plant

[1] Current address: Center for Biotechnology/Department of Biochemistry, University of Wisconsin, Madison, WI 53706.
[2] Current address: Department of Genetics, University of Wisconsin, Madison, WI 53706.
[3] Current address: Keck School of Medicine, University of Southern California, Los Angeles, CA 90033.
[4] To whom correspondence should be addressed. E-mail bartel@rice.edu; fax 713-348-5154.

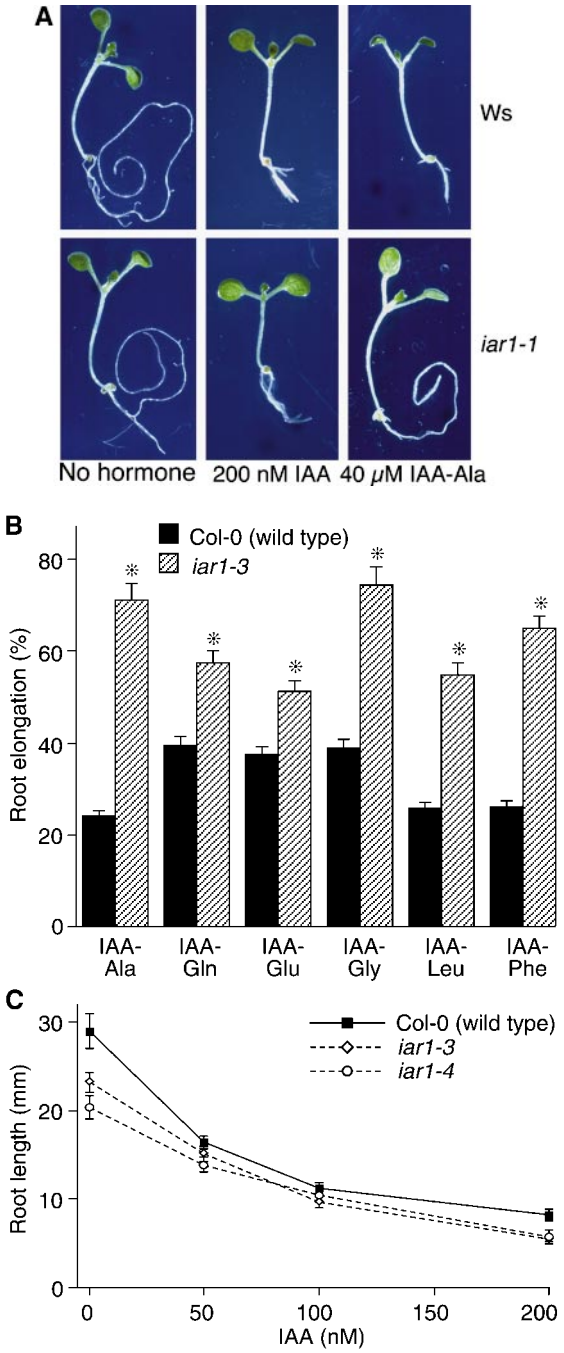

Figure 1. *iar1* Roots Have Decreased Sensitivity to IAA–Amino Acid Conjugates and Normal Sensitivity to IAA.

(A) Eight-day-old *iar1-1* mutant and Wassilewskija (Ws) wild-type seedlings were removed from the agar and photographed after growth on medium containing no hormone, 200 nM IAA, or 40 μM IAA-Ala.

(B) Wild-type Columbia (Col-0) and *iar1* mutant seed were plated on medium containing 20 μM of the indicated IAA–amino acid conjugates. After 8 days, the primary root of each seedling was measured and normalized against growth on unsupplemented medium. Error bars indicate standard errors of the means ($n = 13$), and asterisks indicate significant differences from the wild type (Student's t test, $P < 0.0001$).

(C) Wild-type (Col-0) and *iar1* mutant seed were plated on medium containing the indicated concentrations of IAA. After 8 days, the primary root of each seedling was measured. Error bars indicate standard errors of the means ($n = 10$).

development. Here, we report the isolation of the *iar1* auxin conjugate–resistant mutant and the positional cloning of *IAR1*, which encodes a polytopic membrane protein with several His-rich regions. IAR1 represents a novel component of the auxin conjugate metabolic machinery in plants, and several possible models for its function are discussed.

RESULTS

Isolation and Characterization of *iar1* Mutants

Certain IAA–amino acid conjugates mimic free IAA in bioassays (reviewed in Bartel, 1997), and IAA conjugates that inhibit Arabidopsis root elongation have been used in mutant screens to identify genes involved in hydrolysis of IAA conjugates (Bartel and Fink, 1995; Davies et al., 1999). We initially identified the *iar1* mutant because its roots elongate at concentrations of IAA-Ala that are normally inhibitory, as shown in Figure 1. Table 1 lists the seven *iar1* alleles, four of which were isolated in screens for IAA-Ala resistance. Three additional *iar1* alleles were identified as enhancers of the *ilr1* mutant, which is defective in an IAA conjugate hydrolase (Bartel and Fink, 1995). These alleles were isolated based on the increased resistance of *ilr1 iar1* double mutants to IAA-Leu or IAA-Phe. The recessive nature of the *iar1* mutations (data not shown) suggests that they are loss-of-function alleles.

We quantitated the IAA conjugate resistance of the *iar1* alleles by comparing root lengths of seedlings grown on medium containing various conjugates. All *iar1* alleles are resistant to IAA-Ala, *iar1-4* and *iar1-5* being the strongest and weakest alleles, respectively (data not shown). Because *ilr1 iar1* double mutants are highly resistant to IAA-Leu and IAA-Phe (data not shown), we tested the response of *iar1* single mutants to these conjugates in root elongation assays. *iar1-3* is resistant to IAA-Phe at all concentrations tested (10 to 40 μM) but is resistant to IAA-Leu only at lower concentrations (10 to 20 μM; Figure 1B and data not shown). *iar1* roots are also resistant to elongation inhibition by IAA-Gly, IAA-Gln, and IAA-Glu (Figure 1B), indicating that IAR1 is re-

Table 1. *iar1* Mutant Alleles

Allele	Accession	Screen	Mutagen	Codon Change[a]	Amino Acid Change	Allele Detection
iar1-1	Ws	IAA-Ala^R	EMS	GGA→AGA	Gly^{400}→Arg	Destroys HpaII site
iar1-2	Ws	IAA-Ala^R	EMS	GGA→AGA	Gly^{423}→Arg	Destroys AciI site
iar1-3	Col-0	IAA-Ala^R	Fast neutron	GGAATG→GGGCCTG	Frameshift at codon 458	Creates HaeIII site
iar1-4	Col-0	IAA-Ala^R	Fast neutron	65 to 80-kb deletion including entire *IAR1* coding region		Late-flowering due to *FKF1* deletion[b]
iar1-5	Ws	*ilr1* enhancer IAA-Leu^R	EMS	AGA→AAA	Arg^{357}→Lys	Sequencing
iar1-6	Ws	*ilr1* enhancer IAA-Leu^R	EMS	CAA→TAA	Gln^{162}→stop	Destroys HphI site
iar1-7	Ws	*ilr1* enhancer IAA-Phe^R	EMS	tagCT→taaCT (3′ splice site of first intron)[c]	Predicted to disrupt splicing	Creates AluI site

[a] Nucleotide changes are underlined.
[b] Nelson et al., 2000.
[c] Intron bases are in lowercase letters; exon bases are in uppercase letters.

quired for IAA conjugate sensitivity in general rather than being conjugate specific. In contrast, *iar1* plants respond normally to a range of concentrations of free IAA (Figures 1A and 1C), indicating that mutations in *IAR1* alter conjugate sensitivity rather than general auxin responsiveness.

As shown in Figure 2, exogenous IAA or IAA conjugates can inhibit Arabidopsis hypocotyl elongation in the light; accordingly, we examined the effects of IAA conjugates on *iar1* hypocotyl elongation. *iar1* mutant hypocotyls respond normally to free IAA but are resistant to the inhibitory effects of IAA-Ala on elongation (Figure 2). These results suggest that IAR1 functions in the hypocotyls as well as the roots of Arabidopsis seedlings.

The *iar1* Mutation Partially Suppresses *alf1* Phenotypes

The Arabidopsis *aberrant lateral root formation* (*alf1*) mutant (Celenza et al., 1995), also isolated as rooty (King et al., 1995), *superroot1* (Boerjan et al., 1995), and *hookless3* (Lehman et al., 1996), overproduces both free and conjugated IAA (Boerjan et al., 1995; King et al., 1995; Lehman et al., 1996). *alf1* plants have short primary roots, display increased numbers of adventitious and lateral roots, fail to make an apical hook when germinated in the dark, and are completely sterile under normal growth conditions (Celenza et al., 1995). These phenotypes can be copied by applying auxin to wild-type plants (Boerjan et al., 1995; Celenza et al., 1995; King et al., 1995; Lehman et al., 1996). To investigate whether IAR1 influences IAA responses in vivo, we generated homozygous *iar1*/*iar1 alf1*/*alf1* plants (see Methods). *iar1* partially rescues the fertility defect of *alf1*, in that double mutants yield some seed. In addition, *iar1 alf1* plants are able to form a partial apical hook when germinated in the dark (data not shown). We quantified the degree to which *iar1* suppresses *alf1* by monitoring root elongation on unsupplemented medium. As shown in Figure 3, the *iar1* mutation suppresses the *alf1* root elongation defect. The observation that loss of *IAR1* function can partially alleviate defects in the *alf1* auxin-overproducing mutant suggests that IAR1 normally acts to increase the concentrations of free IAA or the sensitivity to IAA.

Suppression of the *iar1* Phenotype by Manganese

The Arabidopsis amidohydrolases characterized to date require a metal cofactor. Mn^{2+} and Co^{2+} are the most effective

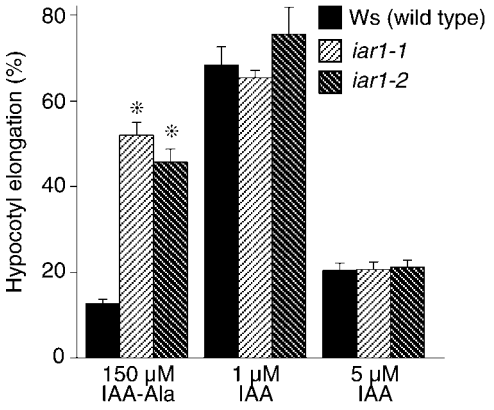

Figure 2. *iar1* Hypocotyls Have Decreased Sensitivity to IAA-Ala.

Wild-type and *iar1* seed were plated on medium containing the indicated concentrations of IAA or IAA-Ala. After 8 days in yellow-filtered light at 22°C, hypocotyls were measured and normalized against growth on unsupplemented medium. Error bars indicate standard errors of the means ($n = 20$ for Ws and *iar1-1*, $n = 9$ for *iar1-2*), and asterisks indicate significant differences from the wild type (Student's *t* test, $P < 0.0001$).

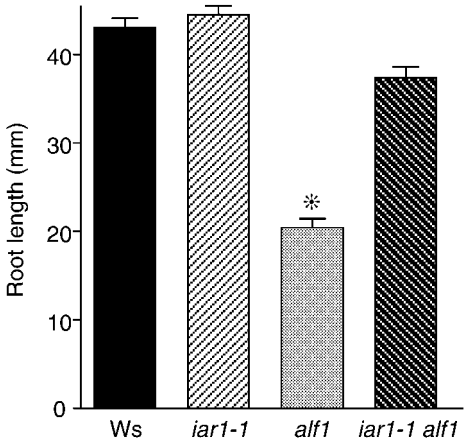

Figure 3. *iar1* Suppresses the *alf1* Root Elongation Defect.

Seed of Ws (wild type), *iar1-1* and *alf1* single mutants, and *iar1-1 alf1* double mutants were plated on unsupplemented medium. After 10 days under yellow-filtered light at 22°C, the primary root of each seedling was measured. Homozygous *alf1* mutants were identified among the progeny of an *alf1/ALF1* parent based on the epinastic cotyledon phenotype. Error bars indicate standard errors of the means ($n \geqslant 18$), and the asterisk indicates a significant difference from the wild type (Student's *t* test, $P < 0.0001$).

cofactors identified for heterologously expressed Arabidopsis IAA–amino acid conjugate hydrolases purified from *Escherichia coli* (Bartel and Fink, 1995; Davies et al., 1999; R. Tellez and B. Bartel, unpublished data). Because mutations in these amidohydrolases can cause IAA–amino acid conjugate resistance (Bartel and Fink, 1995; Davies et al., 1999), mutations that prevent the hydrolases from assembling with or retaining the proper cofactor also might cause this phenotype. We examined the response of *iar1* to Mn^{2+} alone or to IAA-Ala and Mn^{2+}. As shown in Figure 4A, Mn^{2+} alone did not dramatically inhibit root growth at the concentrations tested. However, high Mn^{2+} concentrations partially suppressed the IAA-Ala resistance of *iar1* (Figure 4B). This finding suggests that IAR1 might be necessary to provide the correct metal cofactor to the IAA–amino acid conjugate hydrolases.

IAR1 Cloning

To elucidate the role of IAR1 in conjugate metabolism, we cloned *IAR1* by using a map-based positional approach. A recombination mapping population was prepared by outcrossing *iar1* plants in the Wassilewskija (Ws) accession to wild-type Columbia (Col-0) plants. DNA isolated from IAA-Ala–resistant F_2 progeny was analyzed with polymerase chain reaction (PCR)–based polymorphic markers (Konieczny and Ausubel, 1993; Bell and Ecker, 1994). The *iar1* mutation was localized to an unsequenced (at that time) region at the bottom of chromosome 1, between simple sequence length polymorphism markers nga280 and nga111 (Bell and Ecker, 1994). An 800-kb yeast artificial chromosome (YAC) contig had been described in this interval (Vijayraghavan et al., 1995), and we used subclones from these and other nearby YACs to develop additional PCR-based markers for mapping (see Methods). We localized the *iar1* mutation between the markers 9H12LE and 13A11RE, as shown in Figure 5. Using PCR and DNA hybridization analysis, we determined that this interval is completely contained on the 116-kb bacterial artificial chromosome (BAC) T7E4 (Figure 5A).

We constructed a complementation library from BAC T7E4 (see Methods) and used Agrobacterium to transform (Clough and Bent, 1998) these subclones into the *iar1* mutant. T_2 progeny of *iar1-3* plants transformed with the various constructs were tested for conjugate resistance. Approximately 75% of the T_2 progeny of C37 (Figure 5B) transformants had wild-type IAA-Ala sensitivity, as expected for a rescuing construct. We sequenced the 12-kb insert of C37 and identified several potential coding regions. One of these genes was altered in all seven *iar1* alleles. Three alleles (*iar1-1*, *iar1-2*, and *iar1-5*) had mutations that caused amino acid substitutions; *iar1-6* had a nonsense mutation; the mutation in *iar1-7* probably disrupted splicing because it changed the final G of the first intron to an A; *iar1-3* had a frameshift mutation predicted to replace the last 11 amino acids of IAR1 with an alternative 14–amino acid stretch (Table 1; Figure 5C); and *iar1-4* had an ~65- to 80-kb deletion that included the entire C37 region (Nelson et al., 2000). Finally, the 6.5-kb genomic clone pBIN*IAR1*g (see Methods), which contains the *IAR1* open reading frame with 2.1 kb of DNA upstream of the initiator ATG, completely restored IAA-Ala sensitivity to the *iar1* mutant (Figure 5D), confirming that we had identified *IAR1*.

IAR1 Encodes a Membrane Protein with Multiple His-Rich Regions

We isolated a full-length *IAR1* cDNA (GenBank accession number AF216524) by hybridization to a cDNA library (see Methods). Comparing this cDNA with various genomic sequences revealed that the *IAR1* coding region has 10 introns (Figure 5C) and potentially encodes a 469–amino acid protein with seven or eight transmembrane domains, as shown in Figures 6A and 7. IAR1 is 28% identical to the Drosophila Catsup (catecholamines up) protein (GenBank accession number AAF37226) and 26% identical to the predicted mouse KE4 and human HKE4 proteins (Abe et al., 1988; St.-Jaques et al., 1990; Janatipour et al., 1992; Ando et al., 1996). Uncharacterized IAR1 homologs are found in other multicellular organisms, including Drosophila (GenBank accession numbers AAF49687, AAF50401, and AAF56960), *Caenorhabditis elegans* (GenBank accession numbers CAB17070, CAB05297.1, and CAB02806.1), and zebrafish (GenBank ac-

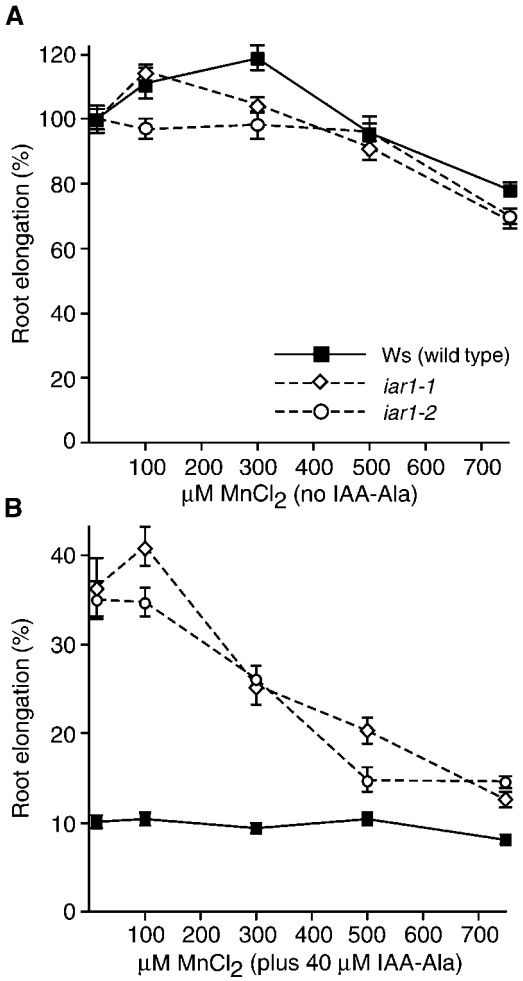

Figure 4. Manganese Suppresses *iar1* IAA-Ala Resistance.

Wild-type (Ws) and *iar1* mutant seed were plated on medium containing 14 to 750 μM manganese either with or without 40 μM IAA-Ala. After 8 days under yellow-filtered light at 22°C, the primary root of each seedling was measured and normalized to growth on unsupplemented medium (which contained 14 μM manganese). Error bars indicate standard errors of the means ($n = 12$).

(A) Without IAA-Ala.

(B) With 40 μM IAA-Ala.

cession number AAF05821). Figure 6A shows an alignment of IAR1 with similar proteins from Drosophila and mammals.

The closest IAR1 homologs of known function are members of the ZIP (ZRT, IRT-like protein) family of metal transporters (Eng et al., 1998; Guerinot and Eide, 1999; Guerinot, 2000), which are ~10 to 13% identical to IAR1 (Figure 6B). These widespread transporters have been characterized from yeast (Zhao and Eide, 1996a, 1996b; MacDiarmid et al., 2000), Arabidopsis (Grotz et al., 1998), and mammals (Lioumi et al., 1999; Gaither and Eide, 2000).

The Mouse *KE4* Gene Can Functionally Substitute for *IAR1* in Arabidopsis

The *IAR1* homologs *KE4* and *HKE4* are mouse and human genes of unknown function (Abe et al., 1988; St.-Jaques et al., 1990; Janatipour et al., 1992; Ando et al., 1996). In addition to 26% amino acid identity (Figure 6A), IAR1 and KE4 share very similar hydropathy plots, suggesting comparable membrane-spanning topologies (Figure 7). To determine whether the Arabidopsis IAR1 and mammalian KE4 proteins function analogously, we transformed *iar1-3* mutant plants with a construct expressing the *KE4* cDNA from the constitutive cauliflower mosaic virus 35S promoter (35S-*MmKE4*). As shown in Figure 8, the 35S-*MmKE4* construct substantially restores IAA-Ala sensitivity to the *iar1* mutant, indicating that the mouse *KE4* gene can substitute for *IAR1* in vivo. This finding suggests that IAR1 and KE4 have similar functions in Arabidopsis and mammals.

Several Arabidopsis *ZIP* genes have been isolated (Grotz et al., 1998) that restore growth on low-zinc medium to a *S. cerevisiae zrt1 zrt2* double mutant that is defective in high- and low-affinity plasma membrane–localized zinc transporters (Zhao and Eide, 1996a, 1996b). We tested whether IAR1 could rescue this mutant because these transporters are apparently related to IAR1 (Figure 6B) and are structurally similar (Figure 7). In contrast to the expression of several Arabidopsis *ZIP* genes (Grotz et al., 1998), *IAR1* expression does not rescue the *zrt1 zrt2* strain in the presence of limiting zinc (data not shown), suggesting that *IAR1* does not encode a plasma membrane–localized zinc transporter. However, perhaps IAR1 does not fold or localize properly in yeast, because the human hZIP2 zinc transporter also fails to rescue *zrt1 zrt2* mutants (Gaither and Eide, 2000).

DISCUSSION

Requirement of *IAR1* for IAA–Amino Acid Conjugate Sensitivity

Phenotypic analysis of *iar1* mutants indicates that IAR1 participates in IAA–amino acid conjugate metabolism or sensing. *iar1* mutant roots and hypocotyls respond normally to free IAA but are less sensitive than wild-type roots and hypocotyls to several IAA–amino acid conjugates (Figures 1 and 2). In contrast, two other IAA–amino acid–resistant mutants, *ilr1* and *iar3*, are defective in IAA conjugate hydrolases that have distinct substrate specificities and display correspondingly restricted conjugate resistance profiles (Bartel and Fink, 1995; Davies et al., 1999). The broad *iar1* conjugate resistance profile suggests a general role for IAR1 in IAA–amino acid conjugate metabolism rather than an IAA-Ala–specific role.

Mutation of *IAR1* partially alleviates several auxin overproduction phenotypes of the *alf1* mutant, indicating that IAR1

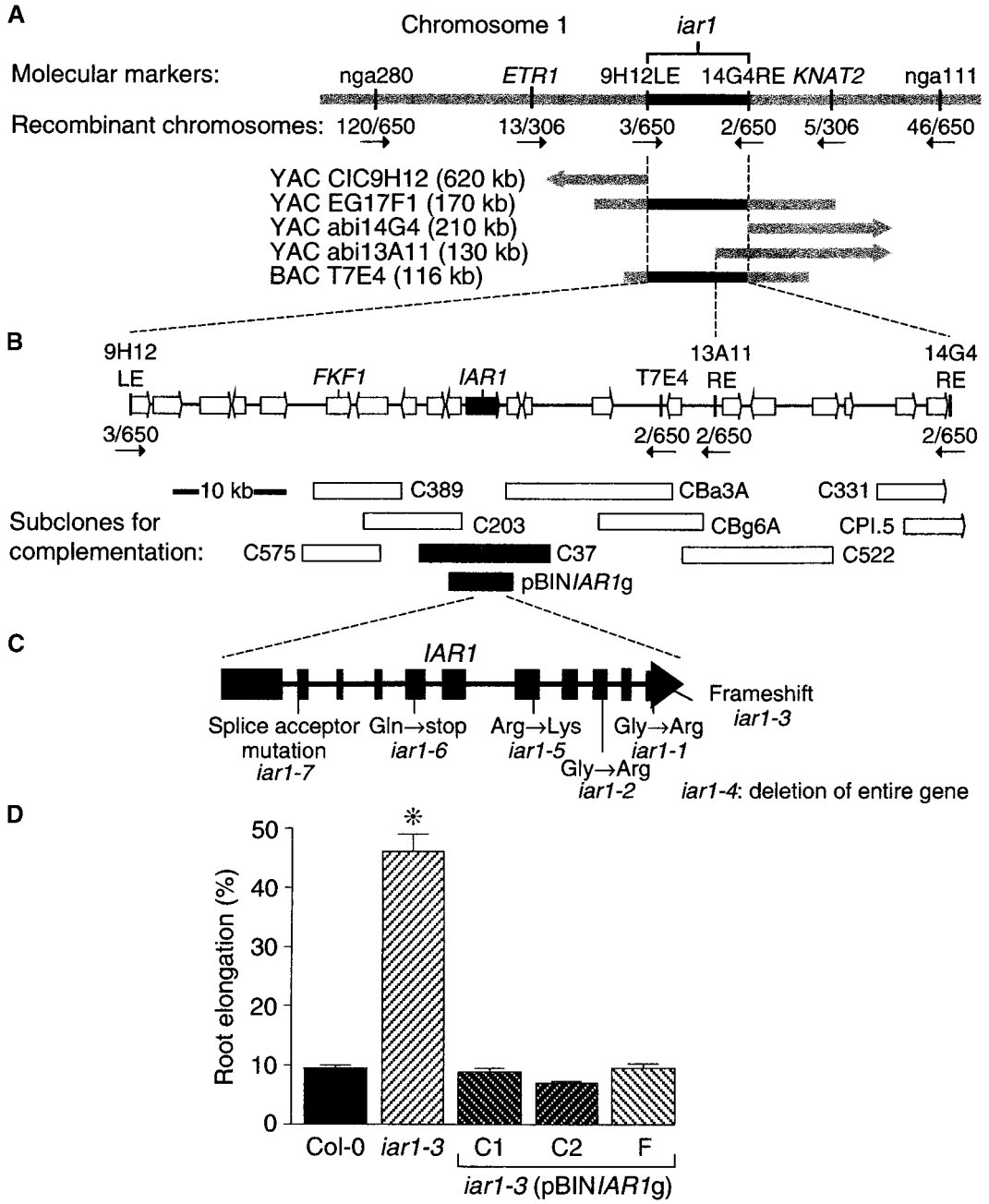

Figure 5. Positional Cloning of *IAR1*.

(A) Recombination mapping with PCR-based markers nga111 and nga280 (Bell and Ecker, 1994) localized *iar1* to the bottom of chromosome 1. This position was refined to between *ETR1* (Chang et al., 1993) and *KNAT2* (Lincoln et al., 1994). Additional markers from nearby YAC clones included 9H12LE and 14G4RE (Nelson et al., 2000) and a marker made from the right end of YAC abi13A11 (see Methods). These three markers hybridized to BAC T7E4 (Choi et al., 1995).

(B) A complementation library was constructed (see Methods) from BAC T7E4, and subclones that were tested for *iar1* complementation are indicated by rectangles below the predicted genes (arrows) in the region. Subclones shown in black rescued the *iar1* IAA-Ala resistance, and those shown in white did not.

(C) Positions of the seven *iar1* mutations are shown below a scheme of the *IAR1* coding region. Exons are indicated by closed rectangles, and introns are represented by lines.

(D) A genomic construct containing the predicted *IAR1* open reading frame controlled by its own promoter rescued the *iar1* mutant phenotype.

normally increases free IAA or sensitivity to IAA. The *alf1* mutant has shortened primary roots, has more adventitious and lateral roots, and is completely sterile (Celenza et al., 1995), probably because of increased concentrations of free IAA (Boerjan et al., 1995; King et al., 1995; Lehman et al., 1996). The *iar1* mutation partially suppresses the *alf1* phenotype, restoring normal root elongation (Figure 3) and partially restoring fertility and the ability to form an apical hook when germinated in the dark (data not shown).

IAR1 Homologs in Other Multicellular Organisms

The *IAR1* gene potentially encodes a 469–amino acid protein that is 26 to 28% identical to the Drosophila Catsup protein and to mammalian KE4 proteins encoded in the major histocompatibility complex (MHC) class II locus (Abe et al., 1988; St.-Jaques et al., 1990; Janatipour et al., 1992; Ando et al., 1996). Interestingly, these *IAR1*-like genes (Figure 6A) probably play similar or identical roles in plants and animals, because expression of the mouse *KE4* cDNA restores normal IAA-Ala sensitivity to *iar1* plants (Figure 8). These proteins all have predicted cleavable N-terminal signal sequences, several regions rich in His residues, and six or seven transmembrane domains (Figure 6A). Their almost identical hydropathy plots (Figure 7) suggest common membrane topologies. IAR1 is most similar to its homologs in and near potential transmembrane domains, and two of the *iar1* point mutations have Arg residues substituted for conserved Glys in predicted transmembrane domains (Figure 6A), an indication that these regions are functionally important.

IAR1 Similarity to the ZIP Family of Metal Transporters

Intriguingly, members of the ZIP family of metal transporters (reviewed by Guerinot and Eide, 1999; Guerinot, 2000) also have N-terminal signal sequences, seven or eight transmembrane domains (Figure 7), and His-rich regions. Although most ZIP family members were isolated as zinc transporters (Zhao and Eide, 1996a, 1996b; Grotz et al., 1998; Gaither and Eide, 2000), results of both direct uptake assays (Eide et al., 1996; Korshunova et al., 1999; Pence et al., 2000) and competition experiments (Grotz et al., 1998; Gaither and Eide, 2000) suggest that ZIPs can have varied substrate specificities. IAR1, KE4, and Catsup have weak identity to the predicted transmembrane domains of ZIP family members (Figure 6C and data not shown), including most of the consensus residues noted previously (Eng et al., 1998). The conserved His residues in transmembrane domains IV and V of the ZIPs that are essential for metal transport in Arabidopsis IRT1 (Rogers et al., 2000) are conserved in IAR1, Catsup, and KE4 (Figure 6C). However, the IAR1 region corresponding to ZIP transmembrane domains IV and V contains only one transmembrane domain, as predicted by the SMART (Schultz et al., 2000) and PSORT (Nakai and Kanehisa, 1992) motif prediction programs. Although these predicted helices are amphipathic in the ZIPs (Eng et al., 1998), this region in IAR1, Catsup, and KE4 contains even more polar residues. Moreover, IAR1 family members share a conserved Pro residue in the region corresponding to transmembrane domain V of the ZIPs (Figure 6C). This region of IAR1 is probably important because the conservative substitution of a Lys for an Arg at position 357 results in the IAA–amino acid conjugate resistance of the *iar1-5* allele and because this region is very similar in IAR1, KE4, and Catsup (Figure 6A).

A striking feature of IAR1 is the presence of several extremely His-rich regions. His represents 17% of the 88 residues between the predicted signal sequence and the first predicted transmembrane domain and 32% of the 40 residues between the second and third transmembrane domains. In addition, the loop between the third and fourth predicted transmembrane domains has seven consecutive His residues (Figure 6A). The Drosophila and mammalian IAR1 homologs are also His-rich in these areas (Figure 6A), suggesting that these residues are important for IAR1 function. Although the membrane topologies of IAR1 and its homologs are unknown, two of these areas flank the third predicted transmembrane domain, indicating that both faces of the membrane should have His-rich regions. Five of these regions in IAR1 are potential metal-binding motifs with the sequence $(HX)_{3-6}$ (Eng et al., 1998; Guerinot and Eide, 1999). Most ZIP family members contain these motifs between their third and fourth predicted transmembrane domains (Eng et al., 1998), and one of the IAR1 repeats is in this position (Figure 6A). Although IAR1 and the ZIPs share only ~10% amino acid identity, this similarity between IAR1 family members and ZIP family members suggests a common evolutionary ancestor (Figure 6B) and also that IAR1 may transport or bind metals.

Figure 5. (continued).

Seed from the wild type (Col-0), the *iar1-3* mutant, and three *iar1-3* transgenic lines homozygous for the pBIN*IAR1*g construct, shown in **(B)**, were plated on medium containing 40 μM IAA-Ala. After 8 days of growth under yellow-filtered light at 22°C, the primary root of each seedling was measured and standardized against growth on unsupplemented medium. Error bars indicate standard errors of the means ($n \geq 17$), and the asterisk indicates a significant difference from the wild type (Student's *t* test, $P < 0.0001$).

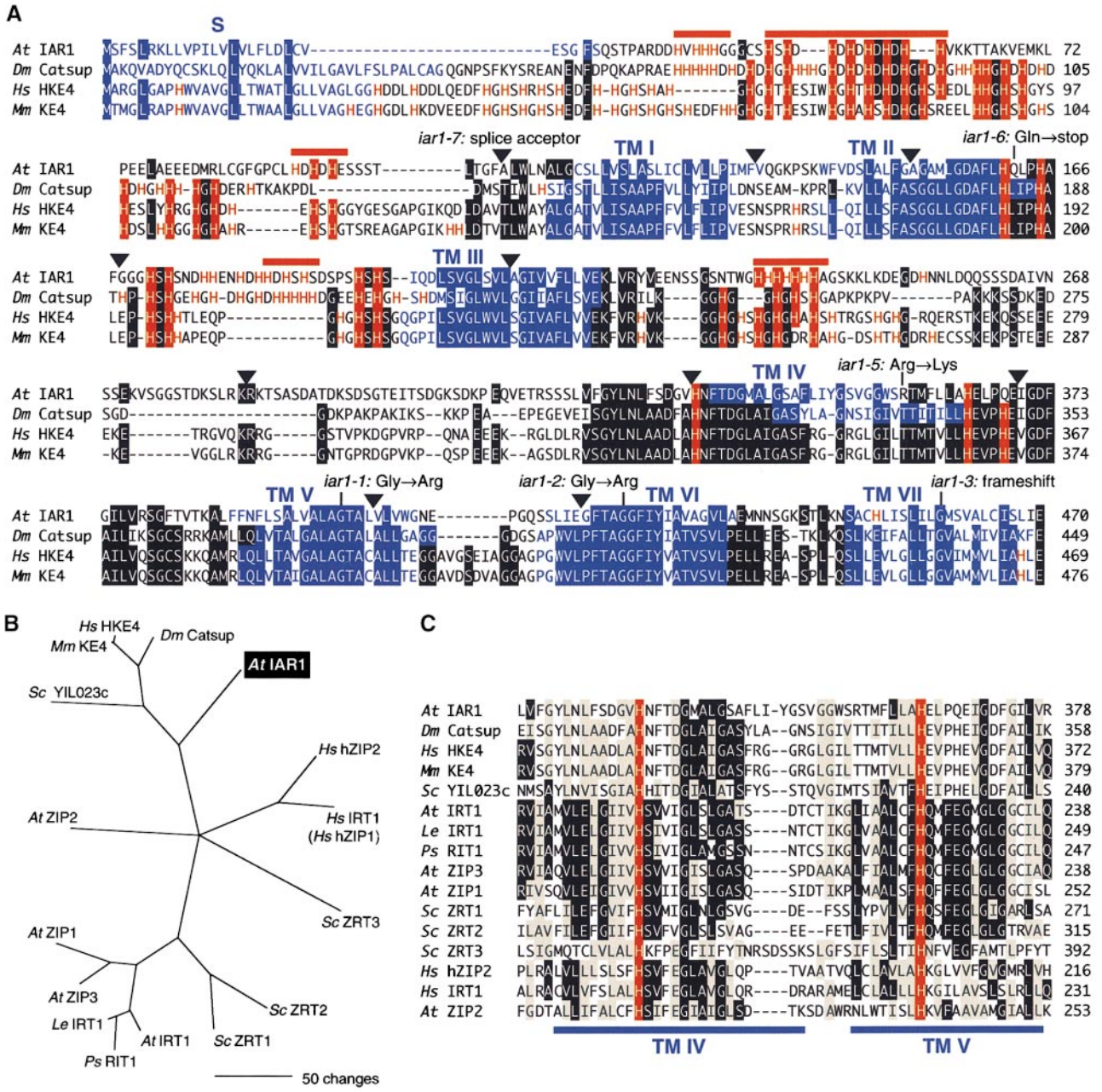

Figure 6. Alignment of IAR1 and Similar Proteins from Other Organisms.

(A) IAR1, Drosophila (*Dm*) Catsup, human (*Hs*) HKE4 (Janatipour et al., 1992; Ando et al., 1996), and mouse (*Mm*) KE4 (Abe et al., 1988; St.-Jaques et al., 1990) predicted proteins were aligned with the Megalign program (DNAStar, Madison, WI) by using the Clustal method (Higgins and Sharp, 1989) with PAM250 residue weights. Residues conserved in at least three proteins are shaded. Triangles indicate the positions of introns in the *IAR1* coding sequence. Positions of *iar1* mutations are shown above the IAR1 sequence, except for *iar1-4*, which is a deletion of the entire *IAR1* gene. The His residues are highlighted in red, and IAR1 potential metal-binding sequences of the type $(HX)_{3-6}$ are indicated by red bars above the sequence. Regions predicted by the SMART program (Schultz et al., 2000) to be transmembrane domains (TM I to VII) are indicated in blue.

(B) Phylogenetic tree of IAR1 and its relatives. The tree reconstructs the evolutionary relationship between IAR1 family members from **(A)** and ZIP proteins, including Arabidopsis (*At*; Korshunova et al., 1999) and tomato (*Le*) IRT1 (GenBank accession number AF136579); pea (*Ps*) RIT1 (GenBank accession number AF065444); Arabidopsis ZIP1, ZIP2, and ZIP3 (Grotz et al., 1998); yeast (*Sc*) ZRT1 (Zhao and Eide, 1996a), ZRT2 (Zhao and Eide, 1996b), ZRT3 (MacDiarmid et al., 2000), and YIL023c (GenBank accession number P40544); and human (*Hs*) IRT1 (hZIP1) and

Possible Roles for IAR1 in IAA Conjugate Metabolism

IAR1 encodes a putative polytopic membrane protein weakly similar to metal transporters. This single-copy gene lacks close Arabidopsis relatives, at least in the sequenced portion of the genome (~98% complete in September 2000; http://arabidopsis.org/agi.html). However, even *iar1* null alleles lack striking morphological phenotypes in the absence of exogenous auxin conjugates, indicating that the plant can compensate for IAR1 deficiency in laboratory growth conditions. Figure 9 presents two models that could explain how the loss of *IAR1* might result in IAA conjugate resistance.

Arabidopsis encodes a family of amidohydrolases, some of which hydrolyze IAA–amino acid conjugates and contain sequence motifs that suggest an endoplasmic reticulum (ER) lumen localization (Bartel and Fink, 1995; Davies et al., 1999). If *IAR1* encodes an ER-localized IAA conjugate transporter, then loss of IAR1 function would prevent conjugates from reaching the hydrolases and would thus cause conjugate resistance. However, we did not detect conjugate transport in microsomes prepared from yeast expressing *IAR1* (data not shown). Additionally, *iar1* rescue by the mouse *KE4* cDNA (Figure 8) indicates that IAR1 and KE4 probably function similarly in plants and mammals. The lack of an obvious need for such a transporter in mammals argues against a direct role for IAR1 in IAA–amino acid conjugate transport.

The shared structural features with the ZIP family of transporters (Figures 6 and 7) suggest that IAR1 might transport a metal. The characterized Arabidopsis amidohydrolases require a metal cofactor, and mutations in these genes can result in IAA–amino acid conjugate resistance (Bartel and Fink, 1995; Davies et al., 1999). Therefore, it is possible that mutations that prevent hydrolases from assembling with or retaining the proper metal might also cause this phenotype. Supplying more of the required cofactor might alleviate IAA–amino acid resistance resulting from such a mutation. This model has precedent in the copper requirement of Arabidopsis ethylene receptors (Rodríguez et al., 1999). Certain copper transporter mutants respond to an ethylene receptor antagonist as if it were ethylene, a phenotype that can be suppressed by providing exogenous copper (Hirayama et al., 1999). Manganese is an effective amidohydrolase cofactor, and the partial suppression of the IAA-Ala resistance of *iar1* by exogenous manganese (Figure 4B) suggests that IAR1 might be an ER-localized manganese transporter. However, *IAR1* expression does not rescue the manganese hypersensitivity of the yeast *pmr1* mutant (data not shown),

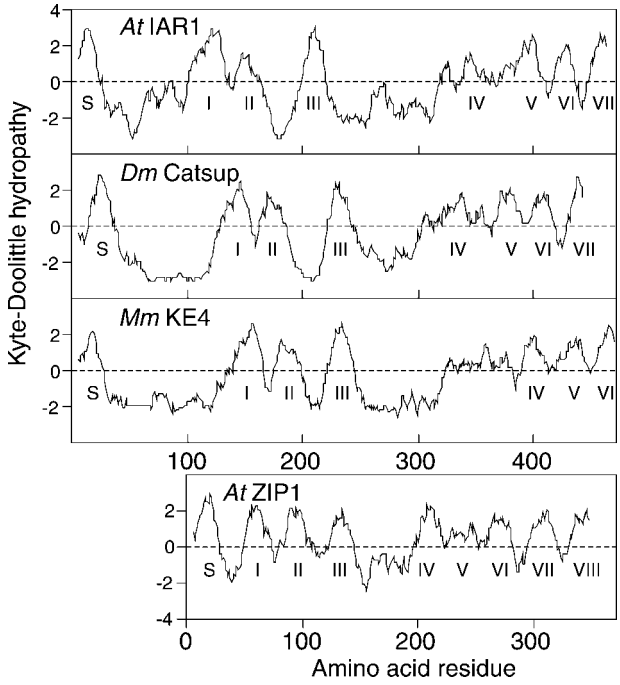

Figure 7. *IAR1* Encodes a Potential Transmembrane Protein.

Hydropathy was calculated for IAR1, Drosophila (*Dm*) Catsup, mouse (*Mm*) KE4 (Abe et al., 1988; St.-Jaques et al., 1990), and Arabidopsis (*At*) ZIP1 (Grotz et al., 1998) with a window size of 13 and a linear weight variation model (Kyte and Doolittle, 1982). Positive and negative values indicate hydrophobic and hydrophilic regions, respectively. Predicted signal sequences are indicated by S, and the transmembrane domains predicted by the SMART program (Schultz et al., 2000) are numbered.

Figure 6. (continued).

hZIP2 (Lioumi et al., 1999; Gaither and Eide, 2000). Sequences (from predicted transmembrane domain IV to the end of the proteins) were aligned as described in **(A)**, and the phylogenetic tree was generated by using PAUP 4.0b3a (Swofford, 2000). The bootstrap method was performed for 100 replicates with a maximum parsimony optimality criterion. All characters were weighted equally. Starting trees for the heuristic search were obtained by random stepwise addition, and tree-bisection-reconnection was the branch-swapping algorithm.

(C) Alignment of predicted transmembrane domains IV and V from the ZIP family members described in **(B)** with the similar region from IAR1 family members. Identical residues and conservative changes seen in at least seven proteins are shown in black and gray boxes, respectively. Transmembrane domains in the ZIP family described by MacDiarmid (2000) are indicated by blue bars below the alignment. The His residues conserved with those in Arabidopsis IRT1 that are required for zinc transport (Rogers et al., 2000) are indicated in red.

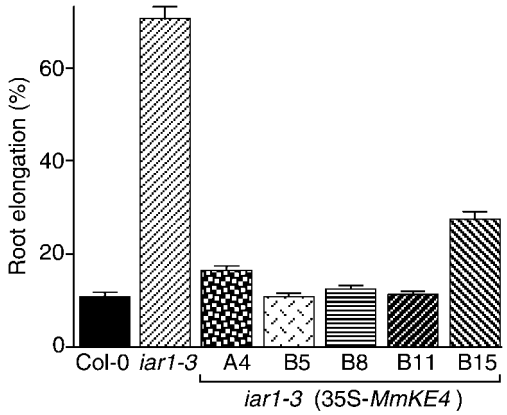

Figure 8. The Mouse *KE4* Gene Can Functionally Substitute for *IAR1*.

Wild-type (Col-0), *iar1-3*, and homozygous T_3 progeny of five independent lines of *iar1-3* plants transformed with 35S-*MmKE4*, a construct containing the mouse *KE4* cDNA (Abe et al., 1988; St.-Jaques et al. 1990) under the control of the cauliflower mosaic virus 35S promoter, were grown for 8 days under yellow-filtered light at 22°C on medium containing 40 μM IAA-Ala. The primary root of each seedling was measured and standardized against growth on unsupplemented medium. Error bars indicate standard errors of the means ($n \geq 20$).

which is defective in an ER-localized calcium and manganese transporter (Rudolph et al., 1989; Dürr et al., 1998). In addition, Arabidopsis ECA1 transports manganese into the ER and rescues the *pmr1* mutant (Liang et al., 1997). Finally, this model would require that the topology of IAR1 in the membrane be reversed compared with that of the ZIPs, which transport metals into the cytoplasm (Eng et al., 1998; Guerinot and Eide, 1999; MacDiarmid et al., 2000). Therefore, we think it unlikely that IAR1 transports manganese into the ER.

A related possibility is that IAR1 exports an inhibitory metal out of the ER. Zinc and copper inhibit the IAR3 amidohydrolase in vitro, even when stoichiometric manganese is present (Lasswell, 2000). Yeast ZRT1 and human hZIP2 are plasma membrane localized (Gitan et al., 1998; Gaither and Eide, 2000), whereas yeast ZRT3 is in the vacuolar membrane, where it appears to mobilize stored zinc in zinc-limited cells (MacDiarmid et al., 2000). Therefore, one could speculate that IAR1 transports zinc, copper, or another inhibitory metal out of the ER and away from the hydrolases (Figure 9A). This model is consistent with the suppression of the *iar1* mutant phenotype by manganese (Figure 4B); excess manganese may outcompete the inhibitory metal from the amidohydrolase and restore activity. It will be interesting to identify the membrane to which IAR1 localizes, because an ER localization would be consistent with this model.

A recent report on the Drosophila Catsup protein (Stathakis et al., 1999), which is ~28% identical to IAR1 (Figure 6A), suggests an alternative role for IAR1 in IAA conjugate responses. The rate-limiting step in catecholamine biosynthesis is the tyrosine hydroxylase (TH)–mediated conversion of L-tyrosine to 3,4-dihydroxy-L-phenylalanine (Kumer and Vrana, 1996). TH is transcriptionally, translationally, and post-translationally regulated (Kumer and Vrana, 1996). *Catsup* mutant flies have normal amounts of TH protein but increased TH activity, which leads to a lethal increase in catecholamine synthesis and suggests that Catsup is a post-transcriptional negative regulator of TH (Stathakis et al., 1999) (Figure 9B). Interestingly, Arabidopsis can hydroxylate IAA conjugates (Östin et al., 1998), perhaps as a mechanism to detoxify excess auxin. Thus, if IAR1 regulates an auxin conjugate hydroxylase the way Catsup regulates TH, increased conjugate hydroxylase activity could explain the IAA–amino acid conjugate resistance of the *iar1* mutant (Figure 9B). A preliminary report suggests that Catsup interacts directly with TH (Burton et al., 2000), so it will be interesting to isolate proteins that physically or geneti-

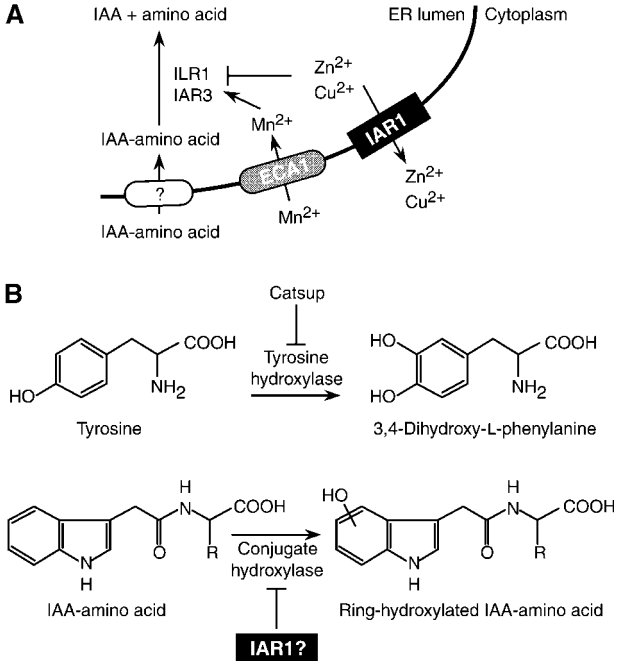

Figure 9. Possible Models for IAR1 Function.

(A) IAR1 may transport inhibitory metals out of the ER. This model is suggested by the weak similarity of IAR1 to ZIP family metal transporters, the suppression of the *iar1* phenotype by the conjugate hydrolase cofactor Mn^{2+}, and the inhibition of conjugate hydrolases by Cu^{2+} or Zn^{2+}.

(B) IAR1 may inhibit an auxin conjugate hydroxylase. This model is suggested by the similarity of IAR1 to the Drosophila tyrosine hydroxylase inhibitor Catsup (Stathakis et al., 1999) and is consistent with the presence of ring-hydroxylated IAA conjugates in plants. Flat-tipped arrows indicate inhibitory interactions. See text for details.

cally interact with IAR1; these may include the targets of IAR1 action in conjugate metabolism.

IAR1 is a novel membrane protein that is involved directly or indirectly in auxin homeostasis. The identification of the *IAR1* gene demonstrates the capacity of genetic screens to uncover unanticipated players in biochemical processes, and the conservation of IAR1 homologs in metazoans suggests that similar proteins play important roles beyond the plant kingdom.

METHODS

Plant Materials and Growth Conditions

Arabidopsis thaliana seed were surface-sterilized (Last and Fink, 1988) and grown on plant nutrient medium (PNS) containing 0.5% sucrose (Haughn and Somerville, 1986) solidified with 0.6% agar. PNS either contained no supplement or was supplemented with 50 nM to 5 μM indole-3-acetic acid (IAA; from a 10 mM stock in ethanol), 20 to 150 μM IAA–amino acid conjugates (from 100 mM stocks in ethanol), 15 μg/mL kanamycin (Kan; from a 25 mg/mL stock in water), 7.5 μg/mL glufosinate-ammonium (BASTA; from a 15 mg/mL stock in 25% ethanol), or 100 to 750 μM $MnCl_2$ (from a 1 M stock in water). IAA and IAA conjugates were from Aldrich (Milwaukee, WI) or were synthesized (S. LeClere and S.P.T. Matsuda, unpublished data). Plates were wrapped in gas-permeable Leukopor surgical tape (Beierdorf Inc., Norwalk, CT) and grown at 22°C in 24-hr illumination under yellow long-pass filters (25 to 45 μE m^{-2} sec^{-1}) to prevent breakdown of indolic compounds (Stasinopoulos and Hangarter, 1990). Plants transferred to soil (Metromix 200; Scotts, Marysville, OH) were grown at 22 to 25°C under continuous illumination (~200 μE m^{-2} sec^{-1}) with Cool White fluorescent bulbs (Sylvania, Versailles, KY).

Mutant Isolation

The *iar1-1* and *iar1-2* mutants were isolated from pools of Wassilewskija (Ws) seed mutagenized with ethyl methanesulfonate (EMS) as described previously (Normanly et al., 1997). Approximately 24,000 surface-sterilized M_2 seed were grown on PNS supplemented with 50 μM IAA-Ala. Two-week-old putative mutants with long roots were transferred to soil and allowed to set seed. The resulting M_3 seed were screened separately for resistance to 50 μM IAA-Ala and for sensitivity to 1 μM IAA. *iar1-3* and *iar1-4* were isolated similarly from M_2 progeny of fast neutron–mutagenized Columbia (Col-0) *gl1-1* seed (purchased from Lehle Seeds, Round Rock, TX). The other alleles were identified from M_2 pools of EMS-mutagenized *ilr1-1* seed on PNS supplemented with 100 μM IAA-Leu (*iar1-5* and *iar1-6*) or 70 μM IAA-Phe (*iar1-7*), as described previously (Davies et al., 1999). The independence of the seven alleles was confirmed by sequencing polymerase chain reaction (PCR) amplification products of genomic DNA. *iar1* mutants were backcrossed at least three times to the parental accession (Col-0 or Ws) before phenotypic analysis.

To obtain the *iar1-1 alf1* homozygous double mutant, an *alf1/ALF1* heterozygous plant (accession Ws) was crossed to the *iar1-1* mutant, and F_2 plants with the phenotypes of both single mutants were transferred to soil and allowed to set seed. Some of these plants were partially fertile (unlike *alf1/alf1 IAR1/IAR1* plants). These plants yielded 100% IAA-Ala–resistant, *alf1*-like progeny, indicating that they were homozygous for both mutations. Root lengths were measured in progeny from these *iar1-1/iar1-1 alf1/alf1* plants after 10 days at 22°C under continuous yellow-filtered light.

Genetic Mapping of *iar1*

To map the *iar1* mutation, we used segregating populations from crosses between *IAR1/IAR1* (accession Col-0) and *iar1/iar1* (accession Ws) plants. Genomic DNA prepared (Celenza et al., 1995) from 325 IAA-Ala–resistant F_2 plants was scored by using published (Konieczny and Ausubel, 1993; Bell and Ecker, 1994; Nelson et al., 2000) and new PCR-based polymorphic markers. New markers developed for mapping include 13A11RE (amplification with the oligonucleotides 5′-GGTCTTCTGTATTTCACATGGC-3′ and 5′-GTGACAATAAGATAATTAGATCCGG-3′ yielded a 144-bp product with one Tsp509I site in Ws and none in Col-0), T7E4 (amplification with the oligonucleotides 5′-CGGTTTCGAGAGTTGCCTCGT-3′ and 5′-GCGAACTGAATAAAAACCTCCG-3′ yielded a 260-bp product with one MseI site in Ws and none in Col-0), *ETR1* (amplification with the oligonucleotides 5′-ATCTCCGTAACCGCTCTTGTCACC-3′ and 5′-ACCACCACCATCTTGTTCCTCTAT-3′ yielded a 1200-bp product with one NcoI site in Ws and none in Col-0), and *KNAT2* (amplification with the oligonucleotides 5′-GGTAGCCATATCAGTTCATTG-3′ and 5′-ATTTAGTTGACACATCAGCTATC-3′ yielded a 660-bp product with three AluI sites in Ws and two in Col-0).

Complementation Library Construction

DNA (~50 μg) from the T7E4 bacterial artificial chromosome (BAC) (Choi et al., 1995) was partially digested with Sau3AI and separated on 0.8% agarose gel containing 1 mM guanosine to prevent UV light damage to the DNA (Gründemann and Schömig, 1996). Fragments of ~10 kb were purified by using the Qiaex II gel extraction kit (Qiagen, Valenica, CA), ligated into a BamHI-digested pBIN19 plant transformation vector (Bevan, 1984), and transformed into *Escherichia coli* strain DH5α. A contig of overlapping clones covering the region in which *iar1* mapped was assembled by using a combination of DNA blot hybridization and sequencing. Selected clones were introduced into *Agrobacterium tumefaciens* GV3101 (Koncz and Schell, 1986) by electroporation (Ausubel et al., 1995). *iar1-1* and *iar1-3* mutant plants were transformed with these constructs by the floral dip method (Clough and Bent, 1998), and Kan-resistant transformants were transferred to soil ~14 days after the T_1 seed had been plated on PNS supplemented with 15 μg/mL Kan. T_2 plants were tested for rescue of the *iar1* IAA-Ala–resistant phenotype by plating on 40 μM IAA-Ala and examining root elongation after 8 days.

pBIN*IAR1*g was made by cloning a 6.5-kb EcoRI fragment from C37 into the EcoRI site of pBIN19. This construct was transformed into *iar1-3* as described above, and homozygous lines were identified by examining the pattern of Kan resistance in the T_3 generation.

To determine the sequences of the various *iar1* mutations, we amplified genomic DNA by PCR with the following pairs of oligonucleotides: 5′-GAGATGCAAAGAGCAACACTC-3′ with 5′-CACTGATGGAATGGCATTAGG-3′, and 5′-CACTGATGGAATGGCATTAGG-3′ with 5′-CTGCAAGAACTCCAGCAACAGCTA-3′ (40 cycles of 15 sec at 94°C, 15 sec at 55°C, and 30 sec at 72°C); and 5′-GAACCAGGACAATCATCGTTG-3′ with 5′-GGTACTGCTATCCAATCCGG-3′, and

5′-CGTGACGATCACGTGCATCATC-3′ with 5′-GCGAATCCGAATGAGAATGATC-3′ (40 cycles of 30 sec at 95°C, 30 sec at 56°C, and 3 min at 72°C). Products were sequenced directly with the primers used for amplification after sequential precipitations with ethanol, polyethylene glycol, and ethanol (Ausubel et al., 1995). The base changes in most *iar1* alleles alter restriction enzyme recognition sites (Table 1).

cDNA Isolation

A full-length *IAR1* cDNA was isolated by hybridizing an Arabidopsis accession Landsberg *erecta* cDNA library (Minet et al., 1992) with a 1.2-kb HindIII/PstI genomic fragment subcloned from the rescuing C37 construct (Figure 5B) containing the last four exons of the *IAR1* gene. The NotI insert of the cDNA was subcloned into the NotI site of pBluescript KS+ (Stratagene, La Jolla, CA) to create KS*IAR1*c, which was sequenced by using vector-derived and internal primers (GenBank accession number AF216524).

Transgenic Lines Expressing the Mouse *KE4* cDNA

A full-length cDNA encoding the mouse IAR1 homolog KE4 in the vector pME18S-FL3 was purchased from Research Genetics (Huntsville, AL). The ~1.6-kb cDNA insert was excised with StuI and XmnI and ligated into the SmaI site of 35SpBARN (S. LeClere and B. Bartel, unpublished data) to create 35S-*MmKE4*, such that the mouse *KE4* cDNA was under the control of the 35S promoter. This construct was transformed into *iar1-3* plants as described above, transformants were selected on PNS supplemented with 7.5 μg/mL BASTA, and homozygous lines were identified by examining the pattern of BASTA resistance in the T_3 generation.

ACKNOWLEDGMENTS

We thank Patrick Masson, John Sedbrook, and Daphne Preuss for sharing markers; John Celenza for *alf1*/*ALF1* seed; Mary Lou Guerinot for the *zrt1 zrt2* yeast strain; Sherry LeClere and Seiichi Matsuda for IAA-Gln and IAA-Glu; Sherry LeClere for 35SpBARN; and Mindy Cohen, Rosie Tellez, and Melanie Stagger for *iar1* alleles. We thank Sherry LeClere, Mónica Magidin, Seiichi Matsuda, and Bethany Zolman for critical comments on the manuscript, and Kevin MacKenzie for helpful discussions. The Arabidopsis Biological Resource Center at The Ohio State University supplied BAC and YAC clones. This research was supported by the National Institutes of Health (Grant No. R29 GM54749), the Robert A. Welch Foundation (Grant No. C-1309), and National Aeronautics and Space Administration/Texas Space Grant Consortium and Houston Livestock Show and Rodeo fellowships (to J.L.).

Received July 31, 2000; accepted October 19, 2000.

REFERENCES

Abe, K., Wei, J.-F., Wei, F.-S., Hsu, Y.-C., Uehara, H., Artzt, K., and Bennett, D. (1988). Searching for coding sequences in the mammalian genome: The H-2K region of the mouse MHC is replete with genes expressed in embryos. EMBO J. **7,** 3441–3449.

Ando, A., Kikuti, Y.Y., Shigenari, A., Kawata, H., Okamoto, N., Shiina, T., Chen, L., Ikemura, T., Abe, K., Kimura, M., and Inoko, H. (1996). cDNA cloning of the human homologues of the mouse *Ke4* and *Ke6* genes at the centromeric end of the human MHC region. Genomics **35,** 600–602.

Ausubel, F., Brent, R., Kingston, R.E., Moore, D.D., Seidman, J.G., Smith, J.A., and Struhl, K. (1995). Short Protocols in Molecular Biology. (New York: John Wiley and Sons).

Bandurski, R.S., Cohen, J.D., Slovin, J.P., and Reinecke, D.M. (1995). Auxin biosynthesis and metabolism. In Plant Hormones, P.J. Davies, ed (Dordrecht, The Netherlands: Kluwer Academic Publishers), pp. 39–65.

Bartel, B. (1997). Auxin biosynthesis. Annu. Rev. Plant Physiol. Plant Mol. Biol. **48,** 51–66.

Bartel, B., and Fink, G.R. (1995). ILR1, an amidohydrolase that releases active indole-3-acetic acid from conjugates. Science **268,** 1745–1748.

Bell, C.J., and Ecker, J.R. (1994). Assignment of 30 microsatellite loci to the linkage map of *Arabidopsis*. Genomics **19,** 137–144.

Bennett, M., Kieber, J., Giraudat, J., and Morris, P. (1998). Hormone regulated development. In Arabidopsis, M. Anderson and J. Roberts, eds (Boca Raton, FL: CRC Press), pp. 107–150.

Bevan, M. (1984). Binary *Agrobacterium* vectors for plant transformation. Nucleic Acids Res. **12,** 8711–8721.

Boerjan, W., Cervera, M.T., Delarue, M., Beeckman, T., Dewitte, W., Bellini, C., Caboche, M., Van Onckelen, H., Van Montagu, M., and Inzé, D. (1995). *superroot*, a recessive mutation in Arabidopsis, confers auxin overproduction. Plant Cell **7,** 1405–1419.

Burton, D.Y., Stathakis, D.G., and O'Donnell, J.M. (2000). The regulation of tyrosine hydroxylase and guanosine triphosphate cyclohydrolase in *Catsup* mutants (abstract no. 751C). In 41st Annual Drosophila Research Conference (Pittsburgh, PA: Genetics Society of America), p. a259.

Campanella, J.J., Ludwig-Müller, J., and Town, C.D. (1996). Isolation and characterization of mutants of *Arabidopsis thaliana* with increased resistance to growth inhibition by indoleacetic acid–amino acid conjugates. Plant Physiol. **112,** 735–745.

Celenza, J.L., Grisafi, P.L., and Fink, G.R. (1995). A pathway for lateral root formation in *Arabidopsis thaliana*. Genes Dev. **9,** 2131–2142.

Chang, C., Kwok, S.F., Bleecker, A.B., and Meyerowitz, E.M. (1993). *Arabidopsis* ethylene-response gene *ETR1*: Similarity of product to two-component regulators. Science **262,** 539–544.

Choi, S., Creelman, R.A., Mullet, J.E., and Wing, R.A. (1995). Construction and characterization of a bacterial artificial chromosome library of *Arabidopsis thaliana*. Weeds World **2,** 17–20.

Clough, S.J., and Bent, A.F. (1998). Floral dip: A simplified method for *Agrobacterium*-mediated transformation of *Arabidopsis thaliana*. Plant J. **16,** 735–743.

Cohen, J.D., and Bandurski, R.S. (1982). Chemistry and physiology of the bound auxins. Annu. Rev. Plant Physiol. **33,** 403–430.

Cohen, J.D., Slovin, J.P., Bialek, K., Chen, K.H., and Derbyshire, M.K. (1988). Mass spectrometry, genetics, and biochemistry: Understanding the metabolism of indole-3-acetic acid. In Bio-

mechanisms Regulating Growth and Development, G.L. Steffens and T.S. Rumsey, eds (Dordrecht, The Netherlands: Kluwer Academic Publishers), pp. 229–241.

Davies, R.T., Goetz, D.H., Lasswell, J., Anderson, M.N., and Bartel, B. (1999). *IAR3* encodes an auxin conjugate hydrolase from Arabidopsis. Plant Cell **11,** 365–376.

Dürr, G., Strayle, J., Plemper, R., Elbs, S., Klee, S.K., Catty, P., Wolf, D.H., and Rudolph, H.K. (1998). The *medial*-Golgi ion pump Pmr1 supplies the yeast secretory pathway with Ca^{2+} and Mn^{2+} required for glycosylation, sorting, and endoplasmic reticulum–associated protein degradation. Mol. Biol. Cell **9,** 1149–1162.

Eide, D., Broderius, M., Fett, J., and Guerinot, M.L. (1996). A novel iron-regulated metal transporter from plants identified by functional expression in yeast. Proc. Natl. Acad. Sci. USA **93,** 5624–5628.

Eng, B.H., Guiernot, M.L., Eide, D., and Saier, M.H. (1998). Sequence analysis and phylogenetic characterization of the ZIP family of metal ion transport proteins. J. Membr. Biol. **166,** 1–7.

Estelle, M., and Klee, H.J. (1994). Auxin and cytokinin in *Arabidopsis*. In *Arabidopsis*, E.M. Meyerowitz and C.R. Somerville, eds (Cold Spring Harbor, NY: Cold Spring Harbor Laboratory Press), pp. 555–578.

Gaither, L.A., and Eide, D.J. (2000). Functional expression of the human hZIP2 zinc transporter. J. Biol. Chem. **275,** 5560–5564.

Gitan, R.S., Luo, H., Rodgers, J., Broderius, M., and Eide, D. (1998). Zinc-induced inactivation of the yeast ZRT1 zinc transporter occurs through endocytosis and vacuolar degradation. J. Biol. Chem. **273,** 28617–28624.

Grotz, N., Fox, T., Connolly, E., Park, W., Guerinot, M.L., and Eide, D. (1998). Identification of a family of zinc transporter genes from *Arabidopsis* that respond to zinc deficiency. Proc. Natl. Acad. Sci. USA **95,** 7220–7224.

Gründemann, D., and Schömig, E. (1996). Protection of DNA during preparative agarose gel electrophoresis against damage induced by ultraviolet light. BioTechniques **21,** 898–903.

Guerinot, M.L. (2000). The ZIP family of metal transporters. Biochim. Biophys. Acta **1465,** 190–198.

Guerinot, M.L., and Eide, D. (1999). Zeroing in on zinc uptake in yeast and plants. Curr. Opin. Plant Biol. **2,** 244–249.

Haughn, G.W., and Somerville, C. (1986). Sulfonylurea-resistant mutants of *Arabidopsis thaliana*. Mol. Gen. Genet. **204,** 430–434.

Higgins, D.G., and Sharp, P.M. (1989). Fast and sensitive multiple sequence alignments on a microcomputer. Comput. Appl. Biosci. **5,** 151–153.

Hirayama, T., Kieber, J.J., Hirayama, N., Kogan, M., Guzman, P., Nourizadeh, S., Alonso, J.M., Dailey, W.P., Dancis, A., and Ecker, J.R. (1999). RESPONSIVE-TO-ANTAGONIST1, a Menkes/Wilson disease–related copper transporter, is required for ethylene signaling in *Arabidopsis*. Cell **97,** 383–393.

Jakubowska, A., Kowalczyk, S., and Leznicki, A.J. (1993). Enzymatic hydrolysis of 4-*O*- and 6-*O*-indol-3-ylacetyl—D-glucose in plant tissues. J. Plant Physiol. **142,** 61–66.

Janatipour, M., Naumov, Y., Ando, A., Sugimura, K., Okamoto, N., Tsuji, K., Abe, K., and Inoko, H. (1992). Search for MHC-associated genes in human: Five new genes centromeric to HLA-DP with yet unknown functions. Immunogenetics **35,** 272–278.

King, J.J., Stimart, D.P., Fisher, R.H., and Bleecker, A.B. (1995). A mutation altering auxin homeostasis and plant morphology in Arabidopsis. Plant Cell **7,** 2023–2037.

Koncz, C., and Schell, J. (1986). The promoter of the T_L-DNA gene 5 controls the tissue-specific expression of chimaeric genes carried by a novel type of *Agrobacterium* binary vector. Mol. Gen. Genet. **204,** 383–396.

Konieczny, A., and Ausubel, F.M. (1993). A procedure for mapping *Arabidopsis* mutations using co-dominant ecotype-specific PCR-based markers. Plant J. **4,** 403–410.

Korshunova, Y.O., Eide, D., Clarke, W.G., Guerinot, M.L., and Pakrasi, H.B. (1999). The IRT1 protein from *Arabidopsis thaliana* is a metal transporter with a broad substrate range. Plant Mol. Biol. **40,** 37–40.

Kowalczyk, S., and Bandurski, R.S. (1990). Enzymatic hydrolysis of 1-*O*-, 4-*O*-, and 6-*O*-indol-3-ylacetyl—D-glucose and the enzymatic synthesis of indole-3-acetyl glycerol by a hormone metabolizing complex. Plant Physiol. **94,** 4–12.

Kuleck, G.A., and Cohen, J.D. (1993). An indole-3-acetyl amino acid hydrolytic enzyme from carrot cells. Plant Physiol. **102** (suppl.), 60.

Kumer, S.C., and Vrana, K.E. (1996). Intricate regulation of tyrosine hydroxylase activity and gene expression. J. Neurochem. **67,** 443–462.

Kyte, J., and Doolittle, R.F. (1982). A simple method for displaying the hydropathic character of a protein. J. Mol. Biol. **157,** 105–132.

Lasswell, J. (2000). Genetic analyses of auxin metabolism and of the transition to flowering in the model plant *Arabidopsis thaliana*. Ph.D. Dissertation (Houston, TX: Rice University).

Last, R.L., and Fink, G.R. (1988). Tryptophan-requiring mutants of the plant *Arabidopsis thaliana*. Science **240,** 305–310.

Lehman, A., Black, R., and Ecker, J.R. (1996). *HOOKLESS1*, an ethylene response gene, is required for differential cell elongation in the Arabidopsis hypocotyl. Cell **85,** 183–194.

Liang, F., Cunningham, K.W., Harper, J.F., and Sze, H. (1997). ECA1 complements yeast mutants defective in Ca^{2+} pumps and encodes an endoplasmic reticulum–type Ca^{2+}-ATPase in *Arabidopsis thaliana*. Proc. Natl. Acad. Sci. USA **94,** 8579–8584.

Lincoln, C., Long, J., Yamaguchi, J., Serikawa, K., and Hake, S. (1994). A *knotted1*-like homeobox gene in Arabidopsis is expressed in the vegetative meristem and dramatically alters leaf morphology when overexpressed in transgenic plants. Plant Cell **6,** 1859–1876.

Lioumi, M., Ferguson, C.A., Sharpe, P.T., Freeman, T., Marenholz, I., Mischke, D., Heizmann, C., and Ragoussis, J. (1999). Isolation and characterization of human and mouse *ZIRTL*, a member of the IRT1 family of transporters, mapping within the epidermal differentiation complex. Genomics **62,** 272–280.

Ludwig-Müller, J., Epstein, E., and Hilgenberg, W. (1996). Auxin-conjugate hydrolysis in Chinese cabbage: Characterization of an amidohydrolase and its role during infection with clubroot disease. Physiol. Plant. **97,** 627–634.

MacDiarmid, C.W., Gaither, L.A., and Eide, D. (2000). Zinc transporters that regulate vacuolar zinc storage in *Saccharomyces cerevisiae*. EMBO J. **19,** 2845–2855.

Minet, M., Dufour, M.-E., and Lacroute, F. (1992). Complementation of *Saccharomyces cerevisiae* auxotrophic mutants by *Arabidopsis thaliana* cDNAs. Plant J. **2,** 417–422.

Monteiro, A.M., Crozier, A., and Sandberg, G. (1988). The biosynthesis and conjugation of indole-3-acetic acid in germinating seed and seedlings of *Dalbergia dolchipetala*. Planta **174,** 561–568.

Nakai, K., and Kanehisa, M. (1992). A knowledge base for predicting protein localization sites in eukaryotic cells. Genomics **14,** 897–911.

Nelson, D.C., Lasswell, J., Rogg, L.E., Cohen, M.A., and Bartel, B. (2000). *FKF1*, a clock-controlled gene that regulates the transition to flowering in *Arabidopsis*. Cell **101,** 331–340.

Normanly, J. (1997). Auxin metabolism. Physiol. Plant. **100,** 431–442.

Normanly, J., and Bartel, B. (1999). Redundancy as a way of life: IAA metabolism. Curr. Opin. Plant Biol. **2,** 207–213.

Normanly, J., Grisafi, P., Fink, G.R., and Bartel, B. (1997). Arabidopsis mutants resistant to the auxin effects of indole-3-acetonitrile are defective in the nitrilase encoded by the *NIT1* gene. Plant Cell **9,** 1781–1790.

Östin, A., Kowalyczk, M., Bhalerao, R.P., and Sandberg, G. (1998). Metabolism of indole-3-acetic acid in Arabidopsis. Plant Physiol. **118,** 285–296.

Pence, N.S., Larsen, P.B., Ebbs, S.D., Letham, D.L.D., Lasat, M.M., Garvin, D.F., Eide, D., and Kochian, L. (2000). The molecular physiology of heavy metal transport in the Zn/Cd hyperaccumulator *Thlaspi caerulescens*. Proc. Natl. Acad. Sci. USA **97,** 4956–4960.

Rodríguez, F.I., Esch, J.J., Hall, A.E., Binder, B.M., Schaller, G.E., and Bleecker, A.B. (1999). A copper cofactor for the ethylene receptor ETR1 from *Arabidopsis*. Science **283,** 996–998.

Rogers, E.E., Eide, D.J., and Guerinot, M.L. (2000). Altered selectivity in an *Arabidopsis* metal transporter. Proc. Natl. Acad. Sci. USA **97,** 12356–12360.

Rudolph, H.K., Antebi, A., Fink, G.R., Buckley, C.M., Dorman, T.E., LeVitre, J., Davidow, L.S., Mao, J., and Moir, D.T. (1989). The yeast secretory pathway is perturbed by mutations in *PMR1*, a member of a Ca^{2+}-ATPase family. Cell **58,** 133–145.

Schultz, J., Copley, R.R., Doerks, T., Ponting, C.P., and Bork, P. (2000). SMART: A web-based tool for the study of genetically mobile domains. Nucleic Acids Res. **28,** 231–234.

Stasinopoulos, T.C., and Hangarter, R.P. (1990). Preventing photochemistry in culture media by long-pass light filters alters growth of cultured tissues. Plant Physiol. **93,** 1365–1369.

Stathakis, D.G., Burton, D.Y., McIvor, W.E., Krishnakumar, S., Wright, T.R.F., and O'Donnell, J.M. (1999). The catecholamines up (Catsup) protein of *Drosophila melanogaster* functions as a negative regulator of tyrosine hydroxylase activity. Genetics **153,** 361–382.

St.-Jaques, B., Han, T.-H., MacMurray, A., and Shin, H.-S. (1990). A putative transmembrane protein with histidine-rich charge clusters encoded in the *H-2K/t*^{w5} region of mice. Mol. Cell. Biol. **10,** 138–145.

Swofford, D.L. (2000). PAUP*: Phylogenetic Analysis Using Parsimony (*and Other Methods). (Sunderland, MA: Sinauer Associates).

Szerszen, J.B., Szczyglowski, K., and Bandurski, R.S. (1994). *iaglu*, a gene from *Zea mays* involved in conjugation of growth hormone indole-3-acetic acid. Science **265,** 1699–1701.

Sztein, A.E., Cohen, J.D., Slovin, J.P., and Cooke, T.J. (1995). Auxin metabolism in representative land plants. Am. J. Bot. **82,** 1514–1521.

Sztein, A.E., Cohen, J.D., García de la Fuente, I., and Cooke, T.J. (1999). Auxin metabolism in mosses and liverworts. Am. J. Bot. **86,** 1544–1555.

Tsurumi, S., and Wada, S. (1986). Dioxindole-3-acetic acid conjugates formation from indole-3-acetylaspartic acid in *Vicia* seedlings. Plant Cell Physiol. **27,** 1513–1522.

Tuominen, H., Östin, A., Sandberg, G., and Sundberg, B. (1994). A novel metabolic pathway for indole-3-acetic acid in apical shoots of *Populus tremula* (L.) × *Populus tremuloides* (Michx.). Plant Physiol. **106,** 1511–1520.

Vijayraghavan, U., Siddiqi, I., and Meyerowitz, E. (1995). Isolation of an 800 kb contiguous DNA fragment encompassing a 3.5-cM region of chromosome 1 in *Arabidopsis* using YAC clones. Genome **38,** 817–823.

Zhao, H., and Eide, D. (1996a). The yeast *ZRT1* gene encodes the zinc transporter protein of a high-affinity uptake system induced by zinc limitation. Proc. Natl. Acad. Sci. USA **93,** 2454–2458.

Zhao, H., and Eide, D. (1996b). The *ZRT2* gene encodes the low affinity zinc transporter in *Saccharomyces cerevisiae*. J. Biol. Chem. **271,** 23203–23210.